

What's Next? Predicting Hamiltonian Dynamics from Discrete Observations of a Vector Field

Zi-Yu Khoo¹, Delong Zhang¹, and Stéphane Bressan¹

National University of Singapore. 21 Lower Kent Ridge Rd, Singapore 119077
{khoozy,zhangde1,steph}@comp.nus.edu.sg

Abstract. We present and compare physics-informed methods for predicting the dynamics of Hamiltonian systems from discrete observation of their vector field in phase space. The methods are variants of the regression devices of the multi-layer perceptron and the Gaussian process. Each method is either more or less informed of the Hamiltonian properties of the system. We empirically and comparatively evaluate the different methods on several physical and abstract dynamical systems. We show that information that the system is Hamiltonian can be effectively informed. We show that different methods strike different trade-offs between efficiency and effectiveness for different dynamical systems.

Keywords: trajectory prediction · physics-informed neural network · data analysis · inductive bias · learning bias.

1 Introduction

The prediction of the dynamics of systems is a relevant and crucial task to many applications in domains ranging from physics and chemistry to engineering, environmental sciences, and economics. Dynamical systems theory [25] studies the temporal dynamics or time evolution of systems. The dynamics of a system is captured by the vector field formed by the time derivatives of the variables describing the system's current state. The system evolves along flow lines in the state space. The flow map is the function that, given an initial state and a time interval, outputs the state of the system after the time interval.

Vector fields are continuous, but they are commonly visualised and measured discretely. Figure 1a shows vectors in the vector field of a nonlinear pendulum in its two dimensional phase space with parameters position (angle of the pendulum oscillating in a plane), and momentum (mass multiplied by velocity), and one flow line following the vectors in the vector field. A nonlinear pendulum at an initial position with initial momentum moves along the flow line as time passes.

A Hamiltonian system [23] is a dynamical system governed by Hamilton's equations. The Hamiltonian property indicates the conservation of some quantity, typically the energy in mechanical and physical systems. For the pendulum of Figure 1a, the conserved energy is the sum of the kinetic energy, i.e half the

square of the momentum, and the potential energy, i.e one minus the cosine of the position for a unitary mass pendulum. The value of the Hamiltonian function for each and every state in a phase space, is represented by the heatmap.

We design, present, and evaluate physics-informed methods for the prediction of the dynamics of a system from the observation of its vector field at discrete locations of the state space.

Figure 1b shows the observed samples of the vector field for the non-linear pendulum of Figure 1a. Figure 1c represents the learned vector field and one learned flow line or sequence of consecutive predictions for an initial condition.

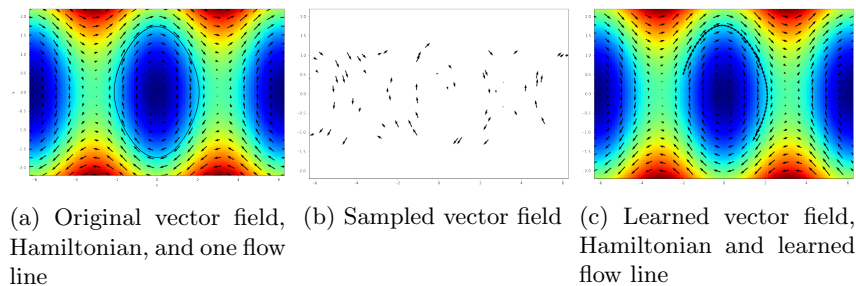


Fig. 1: Phase plots of the nonlinear pendulum

The general method that we present has two consecutive stages. The first stage is the regression of the vector field from the samples. The second stage is the integration of the vector field to calculate the flow map image of a state in the phase space for a prescribed time interval, i.e. the next state on the flow line after the time interval. We show that the information that the system is Hamiltonian can be informed in both stages independently.

However, we want to understand and quantify the significance of this physics information. In the spirit of an ablation study, we compare variants of the general method and different devices with and without the information that the system is Hamiltonian during the first stage, in which a Hamiltonian can be learned under the constraints of Hamilton’s equations, and the second stage, in which symplectic integration can be used, of the general method, respectively.

In addition, the variants in the first stage can be implemented with various regression devices. We consider a multilayer perceptron and a Gaussian process.

We assess the significance of the information that the system is a time independent Hamiltonian system. The empirical comparative performance evaluation is conducted with data from several physical systems of an oscillator, a pendulum, a Henon Heiles system, a Morse potential model of a diatomic molecule, and several abstract systems with logarithmic, inverse trigonometric, exponential, radical and polynomial Hamiltonian functions.

2 Dynamical and Hamiltonian Systems

2.1 Dynamical Systems

Dynamical systems theory [25] studies the temporal dynamics, or time evolution, of systems. Dynamical systems theory defines the instantaneous possible states as the combination of real values of the $2 \times n$ system's state variables, also called degrees of freedom, coordinates, or parameters. Physics notations conventionally evenly split the set of variables into two sets called generalised variables and noted q , for position, and p , for momentum. For the sake of generality, we shall consider an even number of state variables split into two generalised variables noted x and y instead. The phase space, or state space, is the multidimensional space, $\Sigma = \mathbb{R}^{2 \times n}$, with a dimension, or axis, for each state variable.

Without loss of generality, we consider autonomous systems. The dynamics of an autonomous system is captured by the vector field [34,15], $F : \Sigma \rightarrow \mathbb{R}^{2 \times n}$, formed by the time derivatives of the $2 \times n$ state variables. The vector is time independent. In the phase space, the system evolves along flow lines, also called integral curves, paths, or trajectories. A vector of the vector field at each possible state in the phase space is tangent to the corresponding flow line [34,15].

The flow map [15] is a function, $\Phi : \mathbb{R} \times \Sigma \rightarrow \Sigma$, corresponding to the family of integral curves of the vector field at each state of Σ defined in Equation 1.

$$\phi(t, x, y) = \int_0^t F(x, y) dt \quad (1)$$

The flow map, given a time interval, t , and an initial state, $\sigma_0 = (x_0, y_0)$, also referred to as the initial conditions, outputs the system's state after the time interval. We write $\Phi(t, \sigma_0) = \Phi_t(\sigma_0)$. Note that $\Phi_{t_1}(\Phi_{t_2}(\sigma_0)) = \Phi_{t_1+t_2}(\sigma_0)$.

2.2 Hamiltonian Systems

A Hamiltonian system [23] is characterised by a smooth, real-valued scalar function of the state variables [34] (without loss of generality, we only consider time-independent Hamiltonian systems) called the Hamiltonian function or simply the Hamiltonian, $H : \eta \rightarrow \mathbb{R}$, and is governed by Hamilton's equations [23], a system of $2 \times n$ differential equations given in Equations 2 and 3 that define the vector field $F(x, y) = \left(\frac{dx}{dt}, \frac{dy}{dt} \right)$ [23,25].

$$\frac{dx}{dt} = \frac{\partial H(x, y)}{\partial y} \quad (2) \quad \frac{dy}{dt} = -\frac{\partial H(x, y)}{\partial x} \quad (3)$$

The flow map can be calculated by integrating the vector field as in Equation 1 or the gradient of the Hamiltonian with respect to the state variables as in Equations 2 and 3. The Hamiltonian property also implies the conservation of the Hamiltonian [23], as expressed in Equation 4, along flow lines. This typically corresponds to the conservation of energy in mechanical physical systems.

$$\frac{dH(x, y)}{dt} = \frac{dy}{dt} \times \frac{\partial H(x, y)}{\partial y} + \frac{dx}{dt} \times \frac{\partial H(x, y)}{\partial x} = 0 \quad (4)$$

Consequently, the vector field of a Hamiltonian system has a symplectic structure [22]. The Lie derivative of the outer product of its components is zero. A corollary of which is given by Liouville's theorem that states that the phase-space volume of a closed surface is preserved under time evolution (see Appendix).

2.3 Examples of Hamiltonian Systems

For the purpose of illustration and for the comparative empirical evaluation of the methods presented, we consider the following four classical mechanics systems: the simple oscillator, the nonlinear pendulum, the Henon Heiles system, and the Morse potential, as well as four abstract Hamiltonians chosen to illustrate various challenges. Note that, in addition to being Hamiltonian, the mechanical systems have a separable Hamiltonian and verify $\frac{dx}{dt} = y$ for unitary mass.

Figure 2 represents the phase plots of the eight systems with the vector fields and the Hamiltonian values. For each plot, red areas of the heatmap have a higher Hamiltonian value, while blue areas have a lower Hamiltonian value indicated by the colour scale. The phase spaces of the mechanical systems are two-dimensional except for the phase space of the Henon Heiles system, which is four-dimensional.

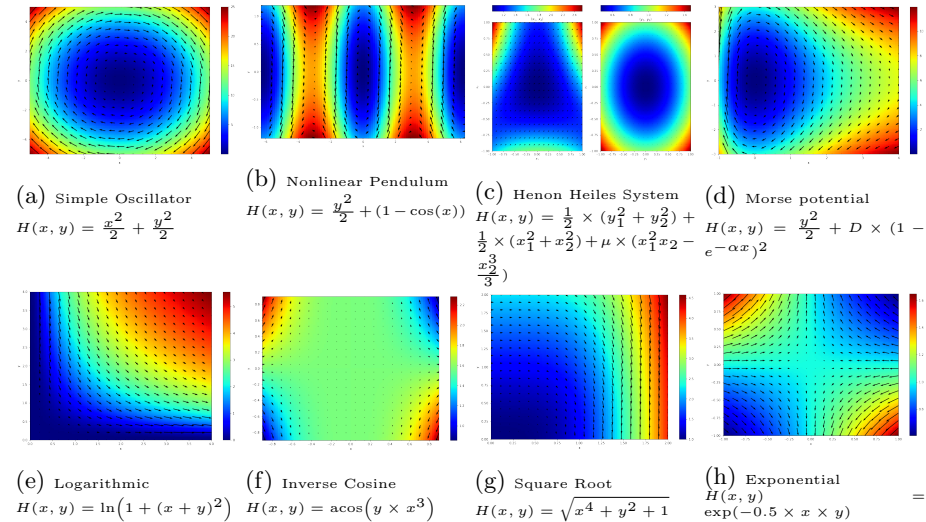


Fig. 2: Phase plots and Hamiltonians of mechanical and abstract systems

3 Related Work

Learning to predict one flow line of a dynamical system from samples of states along that flow line can be addressed as a standard time series prediction problem [4,18]. Modern attempts to solve the time series prediction problem have turned to machine learning methods including recurrent neural networks [13,35,2], long short-term memory recurrent neural networks [14], and neural ordinary differential equations [9,29].

The flow map can be computed from the vector field using an integrator. If the approach ignores that the system is Hamiltonian, it can choose a non-symplectic integrator [5]. If the approach is informed that the system is Hamiltonian, it can use a symplectic integrator such as those introduced by de Vogelaere [33]. Hairer et al. [17] provides a comprehensive introduction to symplectic integrators.

The seminal work of Kantz and Schreiber [21] addresses the problem of learning the flow map from pairs or subsets of states on the same flow lines, referring to it as nonlinear time series analysis. A subset of nonlinear time series analysis is the case when the dynamical system is known to be Hamiltonian. Bertalan et al. [3] use physics-informed machine learning methods to learn the Hamiltonian. Chen et al. [8] directly learn the symplectic flow map. Offen et al. [26] and David et al. [11] use a physics-informed Gaussian process and neural network, respectively, to learn the inverse modified Hamiltonian and vector field, and use a symplectic integrator to compute the flow map. Chen et al. [10] combined the works of Greydanus et al. [16] and Chen et al. [9] to develop a symplectic recurrent multilayer perceptron.

We are interested in the problem of learning the vector field and the flow map from samples of the vector field. There are multiple statistical methods to learn correlated vector-valued functions [7,20,32,36]. Learning vector fields using machine learning has been addressed in the literature under the name of multiple output regression by Hastie et al. [19], state of the art works tackling the problem of supervised learning of the vector field of a dynamical system using neural networks model ordinary differential equations [30] and partial differential equations [31]. Learning vector fields using kernel methods with regularization was introduced by Micchelli et al. [24]. Similarly, Boyle and Frean [6] introduced the use of Gaussian processes to learn vector-valued functions. Recent works focus on the regularization of the vector field, including regularization via spectral filtering [1] and via Tikhonov regularization [37].

Greydanus et al. [16] showed that a physics-informed neural network, similar to Bertalan et al.'s [3], can faster learn the Hamiltonian of mechanical systems and better predict their dynamics from selected samples of their vector fields than a neural network.

Our work addresses the same problem as that of Greydanus et al. [16] while combining ideas from Bertalan et al. [3] and Chen et al. [10].

4 Methodology

4.1 General Method For Predicting the Dynamics from Discrete Observations of the Vector Field

The general method for predicting the dynamics of a system from the observation of its vector field at discrete locations of its phase space comprises two successive stages: the learning or regression of the vector field from the samples and the integration of the vector field into the flow map image of a state in the phase space for a prescribed time interval. We consider four variants of the general methods. They result from the obliviousness or awareness of information that a system is Hamiltonian during the first and second stages of the general method.

We consider two different non-linear regression devices for the learning of a surrogate of the vector field, namely a multilayer perceptron neural network and a Gaussian process. We could potentially choose any other non-linear regression device such as other kernel regression models. The two devices are chosen as the main representatives of parametric and non-parametric non-linear regression statistical machine learning devices. The two devices can learn a surrogate of the vector field. They can, alternatively, learn a surrogate of the Hamiltonian and be used to compute a surrogate of the vector field with automatic differentiation.

4.2 Learning the Vector Field with a Physics-oblivious Surrogate

Let us first consider the supervised learning of a surrogate $\hat{F} = \left(\frac{\hat{d}x}{dt}, \frac{\hat{d}y}{dt}\right)$ of the vector field F with either of two devices: a multilayer perceptron and a Gaussian process. A training data set Z comprises N samples, $\frac{dx}{dt}$ and $\frac{dy}{dt}$, of the vector field for N states (x, y) in the phase space of the system studied. The devices regress the vector-valued function oblivious to any information, other than that embedded in the training data, that the system is Hamiltonian. The devices are trained or fitted to minimise the error between the vectors in the training set and the surrogate output for the corresponding states.

When the surrogate is a multilayer perceptron, its loss function is Equation 5, which is the mean squared error between the approximated vector field and the groundtruth vector field.

$$\left(\frac{\hat{d}x}{dt} - \frac{dx}{dt}\right)^2 + \left(\frac{\hat{d}y}{dt} - \frac{dy}{dt}\right)^2 \quad (5)$$

When the surrogate is a Gaussian process, it uses a Gaussian covariance kernel $k(z, z') = \exp(-\|z - z'\|^2/\epsilon^2)$ where z and z' are states in the phase space, and Z is a collection of states z . ϵ is the kernel width hyperparameter. Equation 6 is the conditional expectation of the Gaussian process $\left(\frac{\hat{d}x}{dt}, \frac{\hat{d}y}{dt}\right)$ at a new state z^* , where $[k(Z, Z')]_{i,j} := k(z_i, z_j)$ is the kernel matrix evaluated over all z values in Z .

$$\mathbb{E}[\hat{V}(z^*)|Z, V(z)] = k(z^*, Z)^\top k(Z, Z')^{-1}V(Z) \quad (6)$$

4.3 Learning the Hamiltonian with a Physics-informed Surrogate and Deriving the Vector Field

Let us now consider learning a surrogate \hat{H} that is an estimator of the Hamiltonian H through unsupervised learning (or semi-supervised learning as the training vectors are used in the loss function instead) from the same training data set Z under the constraints that the system is Hamiltonian. We adapt the method proposed by [3] for learning the Hamiltonian from sample states on flow lines to learning the Hamiltonian and the vector field from samples in the vector field. We use the constraints of Equation 7 to define the loss function of the device. f_0 is an arbitrary pinning term. For cases when the Hamiltonian is the total energy of the system, the arbitrary pinning term encapsulates the assumption that a system at rest has $H_0 = H(x_0, y_0) = 0$ total energy, for $x_0 = 0$ and $y_0 = 0$. In fact, any value can be chosen for H_0 at any chosen state (x_0, y_0) as it only changes the value of the Hamiltonian up to a constant that disappears in the next differentiation step. f_1 and f_2 are Hamilton's equations corresponding to Equation 2 and 3, respectively. They are necessary. f_3 is an additional Hamiltonian conservation property corresponding to Equation 4.

$$\begin{aligned} f_0 &= \left(\hat{H}(x_0, y_0) - H_0 \right)^2 & f_1 &= \left(\frac{\partial \hat{H}}{\partial y} - \frac{dx}{dt} \right)^2 \\ f_2 &= \left(\frac{\partial \hat{H}}{\partial x} + \frac{dy}{dt} \right)^2 & f_3 &= \left(\frac{\partial \hat{H}}{\partial x} \frac{dx}{dt} + \frac{\partial \hat{H}}{\partial y} \frac{dy}{dt} \right)^2 \end{aligned} \quad (7)$$

When the surrogate for the Hamiltonian is a multilayer perceptron neural network, Equation 8 defines the loss function, f , of the multilayer perceptron as a linear combination of the constraints. Training the multilayer perceptron with the states and vectors in Z minimises the loss function minimised by gradient descent along the Hamiltonian spectrum with respect to state variables.

$$f(x, y, \frac{dx}{dt}, \frac{dy}{dt}; w) = \sum_{k=0}^4 c_k f_k \quad (8)$$

When the surrogate is a Gaussian process, constraining its loss function requires evaluating the derivative of the Gaussian process. Constraining the Gaussian process to f_0 requires that the kernel at $z_0 = (x_0, y_0)$ equals H_0 as shown in Equation 9.

$$k(z_0, Z)^\top k(Z, Z')^{-1} H(Z) = H_0 \quad (9)$$

Equation 10 is the derivative of the conditional expectation of \hat{H} with respect to the (new) state z^* .

$$\frac{\partial}{\partial z^*} \mathbb{E}[\hat{H}(z^*) | Z, H(Z)] = \frac{\partial}{\partial z^*} k(z^*, Z)^\top (k(Z, Z')^{-1} H(Z)) \quad (10)$$

Constraining Equation 10 by f_1 and f_2 requires equating the derivative of the surrogate at a state in the phase space, z_i to the vector field. This can be expressed as the conditional expectation of the Hamiltonian shown in Equation 11 where $g(z_i)$ is the vector field at z_i .

$$\frac{\partial}{\partial z} \mathbb{E}[\hat{H}(z_i)|Z] = \frac{\partial}{\partial z_i} k(z_i, Z)^\top (k(Z, Z')^{-1} H(Z)) = g(z_i) \quad (11)$$

Constraining Equation 10 by f_3 requires equating the derivative of the Hamiltonian at one state, z_j , in the phase space, with respect to another state, z_i , to 0, as shown in Equation 12.

$$\frac{\partial}{\partial z} \mathbb{E}[\hat{H}(z_j)|Z] = \frac{\partial}{\partial z_i} k(z_j, Z)^\top (k(Z, Z')^{-1} H(Z)) = 0 \quad \forall z_j \in Z \text{ s.t. } j \neq i \quad (12)$$

Combining Equations 9, 11 and 12 results in Equation 13.

$$\begin{bmatrix} \frac{\partial}{\partial z_1} k(z_1, Z)^\top k(Z, Z')^{-1} \\ \frac{\partial}{\partial z_2} k(z_2, Z)^\top k(Z, Z')^{-1} \\ \vdots \\ \frac{\partial}{\partial z_N} k(z_N, Z)^\top k(Z, Z')^{-1} \\ k(z_0, Z)^\top k(Z, Z')^{-1} \end{bmatrix} [H(Z)] = \begin{bmatrix} g(Z) \\ H_0 \end{bmatrix} \quad (13)$$

Finally, whether the surrogate Hamiltonian is a multilayer perceptron or a Gaussian process, the derivative of the Hamiltonian at any new state of the phase space can be obtained from the surrogate by automatic differentiation. Following Equations 2 and 3, this is then a surrogate of the vector field.

4.4 Integrating the Vector Field to Predict the Dynamics

As suggested by Equation 1, the flow map can be computed by integrating the vector field. Not considering the information that the system is Hamiltonian, one can use any numerical integrator. For this we consider the classic first order explicit Euler integrator [5]. It requires no information of the dynamical system other than its vector field. The symplectic property of Hamiltonian systems let us choose a symplectic integrator [12]. We consider the implicit symplectic Euler integrator [17]. Interestingly, this integrator becomes automatically explicit as soon as the Hamiltonian learned is separable.

5 Performance Evaluation

5.1 Experimental setup

The multilayer perceptrons and physics-informed multilayer perceptrons are designed with two hidden layers of width 16, and use an Adam optimizer. Both set aside 20% of the training data set for validation based early stopping [28]. All Gaussian processes make use of a Gaussian covariance kernel

$k(\sigma, \sigma') = \exp(-\|\sigma - \sigma'\|^2)\epsilon^2$ where σ and σ' are states in the phase space. The Gaussian covariance kernel has a kernel bandwidth parameter of 2, following the settings by Bertalan et al. [3]. All surrogates are trained in Google Colaboratory. Training data set of size $N = 64, 128, 256, 512, \text{ and } 1024$ are sampled uniformly at random from the vector fields of the eight example systems, respectively. The complete code in python and results for the models discussed are available at github.com/zykhoo/predicting_hamiltonian_dynamics.

The quality of the surrogate vector fields is evaluated Subsection 5.2. We use a testing data set of 20^{2n} vectors at evenly spaced states in the phase space for each system. The mean squared error between the ground truth vectors and approximated vectors for each surrogate is computed. We also record the training times. The experiments are repeated for 20 unique random seeds, and the mean values are reported and compared.

The quality of the prediction of the dynamics is evaluated in Subsection 5.2. We use a testing data set of 5^{2n} evenly spaced states in the phase space for each system and the flow lines integrated from the differential equations of the system with a symplectic Euler integrator for 50 time steps, each with step size $h = 0.1$. The mean squared error between the ground truth flow line and the predicted flow line for each method is computed. We also record the prediction times. The experiments are repeated for 20 unique random seeds, and the mean values are reported and compared.

5.2 Learning the Vector Field

We learn the vector field with two-physics-oblivious methods learning the vector field with a multilayer perceptron and a Gaussian process, respectively, and two physics-informed methods learning the Hamiltonian with a multilayer perceptron and a Gaussian process, respectively, and compute the vector field by automatic differentiation [27].

Figure 3 show the inverse of the vector field approximation mean squared error (x axis) and the inverse of surrogate training time (y axis). The colors blue, orange, green, red and purple represent the training data set sizes of 64, 128, 256, 512 and 1024 respectively. The circle, cross, square and plus symbols represent the Gaussian process (GP), multilayer perceptron (NN), physics-informed Gaussian process (PIGP) and physics-informed multilayer perceptrons (PINN) methods respectively, which are used to learn the vector field.

The vector field approximation error is the mean squared error between the ground truth vector field and the approximated vector field by each method. The training time is the time taken for the validation loss of the multilayer perceptron to converge such that early stopping of the multilayer perceptron occurs, or the time taken to compute the kernel of, then fit a Gaussian process. Plotting the inverse vector field approximation error and the inverse training time creates a Pareto plot. Points on the Pareto front of each plot are the optimal methods in the trade-off between training time and mean squared error in approximating the vector field. The plots are given at different scales for the sake of presentation.

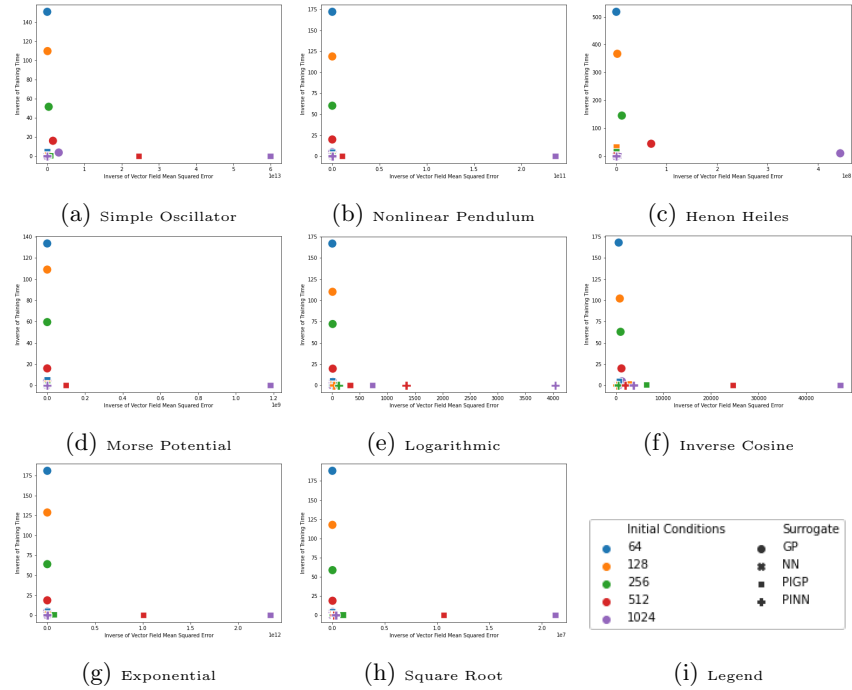


Fig. 3: Learning the vector field

The most efficient method is generally the physics-informed Gaussian process. However, the different methods strike a different compromise between efficiency and effectiveness. The Gaussian process and the physics-informed Gaussian process are on the Pareto front for most systems. The fastest method is the Gaussian process with 64 training data. The method with the lowest mean squared error is the physics-informed Gaussian process with 1024 training data. The remaining methods are clustered at the bottom left of the plot, and dominated by the methods on the Pareto front. For the Logarithmic system, the physics-informed multilayer perceptron has the lowest mean squared error. The physics-informed Gaussian process has higher mean squared error than the physics-informed multilayer perceptron. Figure 4 shows the learned vector fields approximated by the physics-informed methods and the scatter plot of the training data set for the Logarithmic dynamical system. The physics-informed multilayer perceptron has a lower mean squared error than the multilayer perceptron. The multilayer perceptron can better extrapolate the vector field than the Gaussian process.

5.3 Predicting the Dynamics

We predict the dynamics of each Hamiltonian dynamical system by computing the flow map over the interpolated vector field. To compute the flow map, we

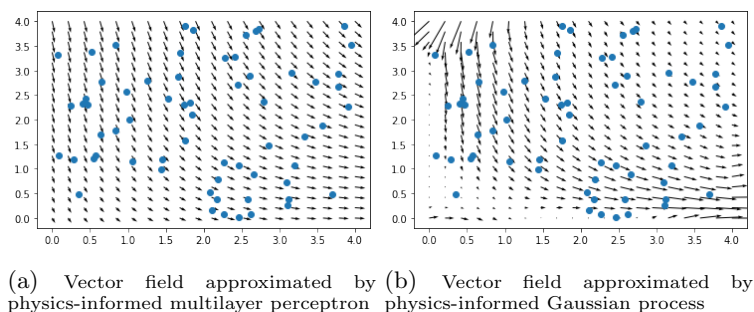


Fig. 4: Vector fields approximated by physics-informed methods and scatter plot in blue of the training data set for Logarithmic dynamical system.

first compute the vector field with the two physics-informed methods above and combine them with either the Euler or symplectic Euler integrator.

Figure 5 shows the inverse prediction error (x axis) and the inverse prediction time (y axis). The colors blue, orange, green, red and purple represent the training data set sizes of 64, 128, 256, 512 and 1024 respectively. The right-pointing triangle, square, down-pointing triangle and empty circle symbols represent the Gaussian process (GPE), physics-informed Gaussian process (PIGPE), multilayer perceptron (NNE), and physics-informed multilayer perceptron (PINNE), all with the Euler integrator. The left-pointing triangle, cross, up-pointing triangle and filled circle symbols represent the Gaussian process (GPSE), physics-informed Gaussian process (PIGPSE), multilayer perceptron (NNSE), and physics-informed multilayer perceptron (PINNSE), all with the symplectic Euler integrator. They learn and integrate the vector field.

The prediction error is the mean squared error between the ground truth flow line and the predicted flow line. The flow line is predicted over 50 time steps, and may include prediction in areas where the vector field is extrapolated. The prediction time is the time taken for the method to compute the vector field at a given state, and compute the next state on the flow line based on the vector field. For the physics-informed Gaussian process, this involves calculating the derivative of the covariance matrix approximating the Hamiltonian. For the physics-informed multilayer perceptron, this involves automatic differentiation [27] of the Hamiltonian with respect to its inputs. Points on the Pareto front of each plot show the optimal methods in the trade-off between prediction time and mean squared error in predicting a flow line. Notice that the plots are given at different scales for the sake of presentation.

The most efficient method is generally the physics-informed multilayer perceptron. However, the different methods strike a different compromise between efficiency and effectiveness. The Gaussian process and physics-informed multilayer perceptron are on the Pareto front for most systems. Methods clustered at the bottom left of the plot are dominated by the those on the Pareto front. The Gaussian process with Euler integrator with 64 training data is the fastest.

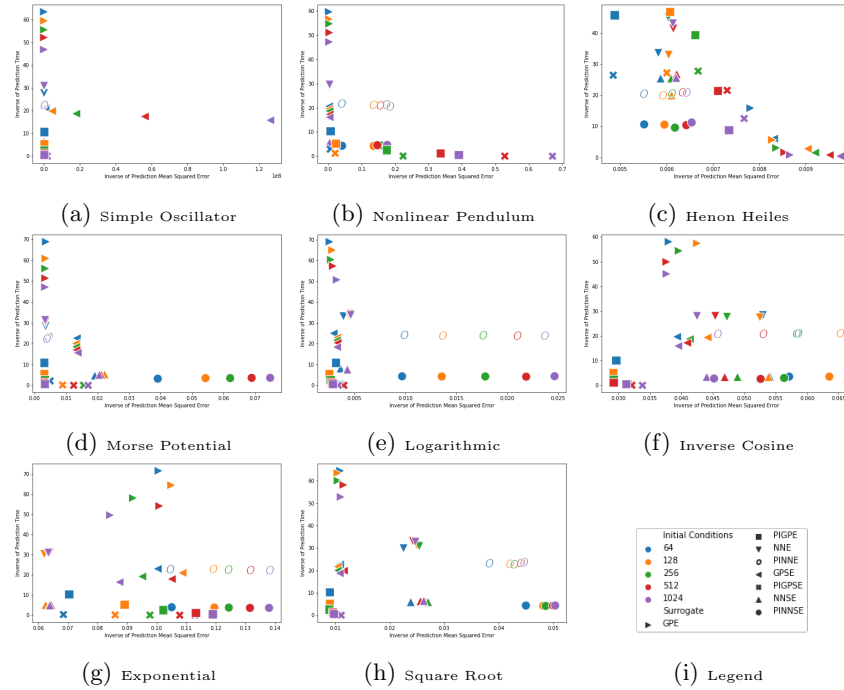


Fig. 5: Predicting the flow map

Generally, the Gaussian process and multilayer perceptron are faster than the physics-informed Gaussian process and physics-informed multilayer perceptron respectively. For the Simple Oscillator, Nonlinear Pendulum and the Henon Heiles system, learning the vector field well translates to the prediction of trajectories. For all other systems, the physics-informed multilayer perceptron has the lowest mean squared error as it is a good extrapolator. For abstract systems, the benefit of the symplectic Euler integrator is marginal, either because the vector field is learned very well, or it extrapolates poorly beyond a threshold. When symplecticity of the vector field is not conserved, the symplectic integrator is counter-productive in predicting flow lines. Methods with symplectic integrators have a longer prediction time than methods with non-symplectic integrators as symplectic integrators are implicit and require iteration for each integration.

6 Conclusion

We design, present, and evaluate physics-informed methods for the prediction of the dynamics of a system from the observation of its vector field at discrete locations of the state space. We show that information that the system is Hamiltonian can be effectively informed in both the regression and integration of the vector field. We show that the physics-informed Gaussian process is generally

more effective for the learning of the vector field while the physics-informed multilayer perceptron is generally more effective for the prediction of the dynamics. However, the different methods strike different trade-offs between efficiency and effectiveness for different dynamical systems.

We are currently investigating the incorporation of additional physics information, for instance that the Hamiltonian is separable and that the system is mechanical, as well as the use of symbolic regression. Preliminary results suggest that these considerations can indeed yield performance improvements.

Acknowledgement

The first author is supported by a scholarship from the Agency of Science, Technology and Research (A*STAR). This research is partially supported by the National University of Singapore (NUS). Any opinions, findings and conclusions or recommendations expressed in this material are those of the author(s) and do not reflect the views of NUS.

References

1. Baldassarre, L., Rosasco, L., Barla, A., Verri, A.: Vector field learning via spectral filtering. In: Balcázar, J.L., Bonchi, F., Gionis, A., Sebag, M. (eds.) *Machine Learning and Knowledge Discovery in Databases*. pp. 56–71. Springer Berlin Heidelberg, Berlin, Heidelberg (2010)
2. Bengio, Y., Simard, P., Frasconi, P.: Learning long-term dependencies with gradient descent is difficult. *IEEE transactions on neural networks* **5**(2), 157–166 (1994)
3. Bertalan, T., Dietrich, F., Mezić, I., Kevrekidis, I.G.: On learning hamiltonian systems from data. *Chaos: An Interdisciplinary Journal of Nonlinear Science* **29**(12), 121107 (Dec 2019)
4. Box, G., Jenkins, G.M.: *Time Series Analysis: Forecasting and Control*. Holden-Day (1976)
5. Boyce, W.E., DiPrima, R.C., Meade, D.B.: *Elementary Differential Equations and Boundary Value Problems*. John Wiley & Sons, 11 edn. (2017)
6. Boyle, P., Frean, M.: Dependent gaussian processes. In: Saul, L., Weiss, Y., Bottou, L. (eds.) *Advances in Neural Information Processing Systems*. vol. 17. MIT Press (2004)
7. Breiman, L., Friedman, J.H.: Predicting multivariate responses in multiple linear regression. *Journal of the Royal Statistical Society: Series B (Statistical Methodology)* **59** (1997)
8. Chen, R., Tao, M.: Data-driven prediction of general hamiltonian dynamics via learning exactly-symplectic maps. In: *International Conference on Machine Learning*. pp. 1717–1727. PMLR (2021)
9. Chen, R.T.Q., Rubanova, Y., Bettencourt, J., Duvenaud, D.K.: Neural ordinary differential equations. In: Bengio, S., Wallach, H., Larochelle, H., Grauman, K., Cesa-Bianchi, N., Garnett, R. (eds.) *Advances in Neural Information Processing Systems*. vol. 31. Curran Associates, Inc. (2018)
10. Chen, Z., Zhang, J., Arjovsky, M., Bottou, L.: Symplectic recurrent neural networks. In: *International Conference on Learning Representations* (2020)

11. David, M., Méhats, F.: Symplectic learning for hamiltonian neural networks. CoRR **abs/2106.11753** (2021)
12. Donnelly, D.P., Rogers, E.L.: Symplectic integrators: An introduction. *American Journal of Physics* **73**, 938–945 (2005)
13. Elman, J.L.: Finding structure in time. *Cognitive Science* **14**(2), 179–211 (1990)
14. Fan, C., Zhang, Y., Pan, Y., Li, X., Zhang, C., Yuan, R., Wu, D., Wang, W., Pei, J., Huang, H.: Multi-horizon time series forecasting with temporal attention learning. In: *Proceedings of the 25th ACM SIGKDD International conference on knowledge discovery & data mining*. pp. 2527–2535 (2019)
15. Frank, J.: *Flow maps and dynamical systems* (December 2008)
16. Greydanus, S., Dzamba, M., Yosinski, J.: Hamiltonian neural networks. In: Wallach, H., Larochelle, H., Beygelzimer, A., d'Alché-Buc, F., Fox, E., Garnett, R. (eds.) *Advances in Neural Information Processing Systems*. vol. 32. Curran Associates, Inc. (2019)
17. Hairer, E., Wanner, G., Lubich, C.: *Symplectic Integration of Hamiltonian Systems*, pp. 179–263. Springer Berlin Heidelberg, Berlin, Heidelberg (2002)
18. Hamilton, J.D.: *Time Series Analysis*. Princeton University Press, 1 edn. (Jan 1994)
19. Hastie, T., Tibshirani, R., Friedman, J.: *The elements of statistical learning: data mining, inference and prediction*. Springer, 2 edn. (2009)
20. Izenman, A.J.: Reduced-rank regression for the multivariate linear model. *Journal of Multivariate Analysis* **5**(2), 248–264 (1975)
21. Kantz, H., Schreiber, T.: *Nonlinear Time Series Analysis*. Cambridge nonlinear science series, Cambridge University Press (2004)
22. Lee, J.M.: *Introduction to smooth manifolds*. Graduate texts in mathematics ;, Springer,, New York : (2003)
23. Meyer, K.R., Hall, G.R.: Hamiltonian Differential Equations and the N-Body Problem, pp. 1–32. Springer New York, New York, NY (1992)
24. Micchelli, C.A., Pontil, M.: On learning vector-valued functions. *Neural Comput* **17**(1), 177–204 (Jan 2005)
25. Nolte, D.D.: The tangled tale of phase space. *Physics Today* **63**, 33–38 (2010)
26. Offen, C., Ober-Blöbaum, S.: Symplectic integration of learned hamiltonian systems. *Chaos: An Interdisciplinary Journal of Nonlinear Science* **32**(1), 013122 (2022)
27. Paszke, A., Gross, S., Massa, F., Lerer, A., Bradbury, J., Chanan, G., Killeen, T., Lin, Z., Gimelshein, N., Antiga, L., Desmaison, A., Kopf, A., Yang, E., DeVito, Z., Raison, M., Tejani, A., Chilamkurthy, S., Steiner, B., Fang, L., Bai, J., Chintala, S.: Pytorch: An imperative style, high-performance deep learning library. In: Wallach, H., Larochelle, H., Beygelzimer, A., d'Alché-Buc, F., Fox, E., Garnett, R. (eds.) *Advances in Neural Information Processing Systems 32*, pp. 8024–8035. Curran Associates, Inc. (2019)
28. Prechelt, L.: Early stopping - but when? In: Orr, G.B., Müller, K.R. (eds.) *Neural Networks: Tricks of the Trade*. Springer Berlin Heidelberg, Berlin, Heidelberg (1998)
29. Rackauckas, C., Ma, Y., Martensen, J., Warner, C., Zubov, K., Supekar, R., Skinner, D., Ramadhan, A.J.: Universal differential equations for scientific machine learning. CoRR **abs/2001.04385** (2020)
30. Raissi, M.: Deep hidden physics models: Deep learning of nonlinear partial differential equations. *J. Mach. Learn. Res.* **19**(1), 932–955 (jan 2018)
31. Ruthotto, L., Haber, E.: Deep neural networks motivated by partial differential equations. *Journal of Mathematical Imaging and Vision* **62**(3), 352–364 (Apr 2020)

32. Van Der Merwe, A., Zidek, J.: Multivariate regression analysis and canonical variates. *Canadian Journal of Statistics* **8**(1), 27–39 (1980)
33. de Vogelaere, R.: Methods of integration which preserve the contact transformation property of the hamilton equations (1956)
34. Wainwright, J., Tenti, G.: Calculus 4 course notes for amath 231 (September 2020)
35. Wan, E.A., et al.: Time series prediction by using a connectionist network with internal delay lines. In: *Santa Fe Institute Studies in the Sciences of Complexity Proceedings*. vol. 15, pp. 195–195. Addison-Wesley publishing co (1993)
36. Wold, S., Ruhe, A., Wold, H., Dunn, III, W.J.: The collinearity problem in linear regression. the partial least squares (pls) approach to generalized inverses. *SIAM Journal on Scientific and Statistical Computing* **5**(3), 735–743 (1984)
37. Zhao, J., Ma, J., Tian, J., Ma, J., Zhang, D.: A robust method for vector field learning with application to mismatch removing. In: *Proceedings of the 2011 IEEE Conference on Computer Vision and Pattern Recognition*. p. 2977–2984. CVPR '11, IEEE Computer Society, USA (2011)

Appendix

Symplectic Integrators

The first-order Euler integrator is the explicit integrator of Equation 14 [17], where $(x_{t+h}, y_{t+h}) = \Phi_h(x_t, y_t) = \Phi_h(\sigma)$. It takes the vector field and multiplies it by the time step h .

$$x_{t+h} = x_t + h \times \frac{dx}{dt} \qquad y_{t+h} = y_t + h \times \frac{dy}{dt} \qquad (14)$$

When the system is Hamiltonian, the outer product of the components of a vector in the vector field is conserved, as illustrated in Equation 15.

$$\frac{d\Phi_h(\sigma)}{d\sigma}{}^T \begin{pmatrix} 0 & -I \\ I & 0 \end{pmatrix} \frac{d\Phi_h(\sigma)}{d\sigma} = \begin{pmatrix} 0 & -I \\ I & 0 \end{pmatrix} \qquad (15)$$

With the information that the system is Hamiltonian, we can use a symplectic integrator like the implicit symplectic Euler integrator of Equation 16 [17].

$$x_{t+h} = x_t + h \times \frac{\partial H(x_t, y_{t+h})}{\partial y_t} \qquad y_{t+h} = y_t - h \times \frac{\partial H(x_t, y_{t+h})}{\partial x_t} \qquad (16)$$